1
The MALDI Process and Method

Franz Hillenkamp and Michael Karas

1.1
Introduction

Matrix-assisted laser desorption/ionization (MALDI) is one of the two "soft" ionization techniques besides electrospray ionization (ESI) which allow for the sensitive detection of large, non-volatile and labile molecules by mass spectrometry. Over the past 15 years, MALDI has developed into an indispensable tool in analytical chemistry, and in analytical biochemistry in particular. This chapter will introduce the reader to the technology as it stands now, and will discuss some of the underlying physical and chemical mechanisms as far as they have been investigated and clarified to date. It will concentrate on the central issues of MALDI, necessary for the user to understand for an efficient application of the technique. An in-depth discussion of these topics would be beyond the scope of this chapter, and hence the reader is referred to recent reviews [1–3]. The details about the current state of instrumentation including the lasers and their coupling to the mass spectrometers will be presented in Chapter 2.

As with most new technologies, MALDI came as a surprise even to the experts in the field on the one hand, but also evolved from a diversity of prior art and knowledge on the other hand. The original notion had been that (bio)molecules with masses in excess of about 500–1000 Da could not be isolated out of their natural (e.g., aqueous) environment, and even less be charged for an analysis in the vacuum of a mass spectrometer without excessive and unspecific fragmentation. During the late 1960s, Beckey introduced *field desorption* (FD), the first technique which opened a small road into the territory of *mass spectrometry* (MS) of bioorganic molecules [4]. Next came *secondary ion mass spectrometry* (SIMS), and in particular static SIMS, introduced by A. Benninghoven in 1975 [5]. This development was taken a step further by M. Barber in 1981 with the introduction of SIMS of organic compounds dissolved in glycerol, which he coined *fast atom bombardment* (FAB). It was in this context, and in conjunction with first attempts to desorb organic molecules with laser irradiation, that the concept of a "matrix" as a means of facilitating desorption and enhancing ion yield was born [6]. The principle of desorption by a bombardment of organic samples with the fission

MALDI MS. A Practical Guide to Instrumentation, Methods and Applications.
Edited by Franz Hillenkamp and Jasna Peter-Katalinić

ISBN: 978-3-527-31440-9

products of the ^{252}Cf nuclear decay, later called *plasma desorption* (PD) was published by R. Macfarlane in 1974 [7]. Subsequently, the groups of Sundqvist and Roepstoff greatly improved the analytical potential of this technique by the addition of nitrocellulose, which not only cleaned up the sample but was also suspected of functioning as a signal-enhancing matrix [8].

The first attempts to use laser radiation to generate ions for a mass spectrometric analysis were published only a few years after the invention of the laser [9–11]. Vastola and Pirone had already demonstrated the spectra of organic compounds, recorded with a time-of-flight (TOF) mass spectrometer. Several groups continued to pursue this line of research, mainly R. Cotter at Johns Hopkins University in the USA and P. Kistemaker at the FOM Institute in Amsterdam, the Netherlands. For a number of years the Amsterdam group held the high mass record for a bioorganic analyte with a spectrum of underivatized digitonin at mass 1251 Da ($[M + Na]^+$), desorbed with a CO_2-laser at a wavelength of 10.6 μm in the far infrared [12].

Independently of and parallel to these groups, Hillenkamp and Kaufmann developed the *laser microprobe mass analyzer* (LAMMA), the commercial version of which was marketed by Leybold Heraeus in Cologne, Germany [13]. The instrument originally comprised a frequency-doubled ruby laser at a wavelength of 347 nm in the near ultraviolet (UV), and later a frequency-quadrupled ND:YAG-laser at a wavelength of 266 nm in the far UV. The laser beam was focused to a spot of <1 μm in diameter to probe thin tissue sections for inorganic and trace atomic ions such as Na, K, and Fe. The mass analyzer of the LAMMA instruments was also a TOF mass spectrometer, and was the first commercial instrument with an ion reflector, which had been invented a few years earlier by B.A. Mamyrin in Leningrad. The sensitivity-limiting "noise" of the LAMMA spectra were signals which were soon identified as coming from the organic polymer used to embed the tissue sections, as well as other organic tissue constituents. It was this background noise which triggered the search for a systematic analysis of organic samples and which eventually led to the discovery of the MALDI principle in 1984. The principle and its acronym were published in 1985 [14] and the first spectrum of the non-volatile bee venom mellitin, an oligopeptide at mass 2845 Da in 1986 [15]. Spectra of proteins with masses exceeding 10 kDa and 100 kDa were published in 1988 [16] and presented at the International Mass Spectrometry Conference in Bordeaux in 1988, respectively.

ESI and MALDI were developed independently but concurrently, and when their potential for the desorption of non-volatile, fragile (bio)molecules was discovered people were mostly impressed by their ability to access the high mass range, particularly of proteins. However, FAB- and PD-MS had at that time already generated spectra of trypsin at mass 23 kDa and other high-mass proteins. What really made the difference in particular for the biologists was the stunning sensitivity which, for the first time, made MS compatible with sample preparation techniques used in these fields. For MALDI, the minimum amount of protein needed for a spectrum of high quality was reduced from 1 pmol in 1988 to a few femtomoles only about a year later. Today, in favorable cases, the level is now down in the low

attomole range. Many other developments – both instrumental (see Chapter 2) as well as specific sample preparation recipes and assays (see other chapters of the book) – took place during the following decade, and the joint impact of all of these together has today made MALDI-MS an indispensable tool not only in the life sciences but also in polymer analysis.

The use of a chemical matrix in the form of small, laser-absorbing organic molecules in large excess over the analyte is at the core of the MALDI principle. Several developments for laser desorption schemes took place in parallel to and following publication of the MALDI principle. These all attempt to replace the chemical matrix by a more easy-to-handle physical matrix, or a more simple combination of the two. The best known of these is the system of Tanaka and coworkers, which was first presented at a Sino-Japanese conference in 1987; details were subsequently published in 1988 [17]. The matrix comprises Co-nanoparticles suspended in glycerol as the basic system into which the analyte is dissolved, similar to the sample preparation of FAB. Several other nano- and micro-particles were tested later, with results comparable to those of Tanaka [18]. For his technique, *surface-assisted laser desorption/ionization* (SALDI), Sunner and co-workers used dry carbon and graphite substrates [19]. Another technique which has found much interest for the analysis of smaller molecules (and which is described in more detail in Chapter 9) was reported by Siuzdak [20]. This method, termed *desorption/ionization on silicon* (DIOS), uses preparations of neat organic samples on porous silicon. Several other methods and acronyms use similar systems such as nanowires or sol-gel systems. All of these methods use the substrate on which the analyte is prepared for the absorption of the laser energy, and are characterized by a sensitivity lower than that of MALDI by several orders of magnitude, as well as a strongly increased ion fragmentation which limits the accessible mass range to somewhere between 2000 and 30 000 Da, depending on the method. There is reason to believe that all of these methods are based on a thermal desorption at the substrate/analyte interface with the high internal excitation of the ions and low ion yield typical for thermal desorption processes. The very high heating and cooling rates, together with high peak temperatures of the substrates as well as the suspension of the absorbers in glycerol, apparently somewhat soften the desorption, the latter most probably through adiabatic cooling in the expanding plume; derivatization of the surfaces can up-concentrate the analyte of interest at the surfaces to increase the sensitivity. Indeed, a yoctomole (10^{-21} mole) sensitivity has been achieved in this way with a perfluorophenyl-derivatized DIOS system for a small hydrophobic peptide [21].

1.2 Analyte Incorporation

What, then is so special about the chemical matrix in MALDI? Some of its important features such as the absorption of the laser energy are easily understood, but surprisingly the overall process of the desorption and ionization has not yet

been fully described, almost 20 years after the invention. As a result, the search for better matrices in general or for specific application still remain mostly empirical.

One important feature is the way in which the matrix and analyte interact in the MALDI sample. In a typical UV-MALDI sample preparation small volumes of an about 10^{-6} M solution of the analyte and a near-saturated (ca. 0.1 M) solution of the matrix are mixed; the solvent is then evaporated before the sample can be introduced into the vacuum of the mass spectrometer. Upon solvent evaporation, the matrix crystallizes to form a bed of small crystals that range in size from a few to a few hundred micrometers, depending on the matrix and the details of the preparation. The typical molar analyte to matrix ratio ranges from about 10^{-2} for small molecules to ca. 10^{-4} for large proteins. The sample preparation is discussed in more detail in Section 1.8. One of the early surprises in the MALDI development was that all of the well-functioning matrices incorporate the analyte in the crystals quantitatively (up to a maximum concentration) and in a homogeneous (on the light microscopic resolution level of 0.5 μm) distribution. This was shown for the UV-MALDI matrices 2,5-dihydroxybenzoic acid (2,5-DHB) [22], sinapinic acid [23] and 4-hydroxy-α-cyanocinnamic acid (HCCA) [24], 3-hydroxy-picolinic acid [24] and the IR-MALDI matrix succinic acid [25]. This homogeneous incorporation, in conjunction with the also homogeneous energy deposition and material ablation (for a discussion, see Section 1.3) result in the co-desorption of intact non-volatile and labile molecules with the matrix and, in addition, to their cooling of internal energy in the expanding plume of material. The mechanisms and driving force for this incorporation are still largely unknown. Horneffer et al. have shown in a systematic study of different position isomers of dihydroxybenzoic acids that only 2,5-DHB incorporates homogeneously and quantitatively, whereas other isomers such as 2,6-DHB do not incorporate at all, while some others incorporate only randomly [26,27]. Confocal laser scan images of the protein avidin, labeled with the fluorochrome Texas red for single crystals of 2,5-DHB and 2,6-DHB are shown in Figure 1.1. No obvious correlation between the incorporation and the crystal structure of these isomers was found. The state of the incorporated analyte molecules in the matrix crystals is another interesting question. Based on results obtained for the incorporation of pH-indicator dye molecules, Krueger et al. have concluded that molecules retain their solution charge state in the crystal, which implies that they also retain their solvation shell [28]. Horneffer et al. have found a high density of cavities of 10–2000 nm size in crystals of both 2,5-DHB and 2,6-DHB by electron microscopy [29]. At first sight, these cavities could be assumed to contain analyte molecules with residual solvent. However, if this is the case it is difficult to understand why 2,5-DHB – but not 2,6-DHB – incorporates analytes into these cavities; attempts to localize gold-labeled protein in the cavities of 2,5-DHB were also inconclusive.

A solventless method for sample preparation was developed originally for the MALDI-MS of synthetic polymers which are often not soluble in standard solvents [30]. In this method, matrix and analyte powders are mixed and ground in a mortar or ball-mill and then applied to a MALDI target support. In a recent report it

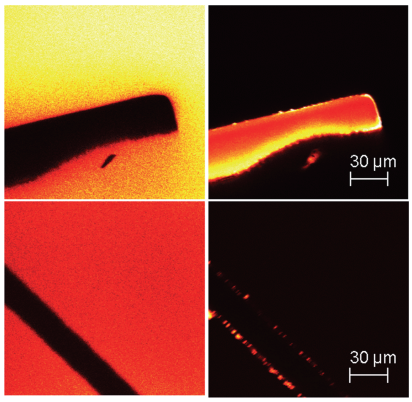

Fig. 1.1 Confocal laser scan fluorescence images of single crystals of 2,5-dihydroxybenzoic acid (top panels) and 2,6-dihydroxybenzoic acid (bottom panels). Both matrices were doped with the protein avidin, labeled with a Texas red (TR) fluorescent dye. The images were recorded at an x,y-plane 12 µm into the crystals. The left panels show dark shadowgraphs of the shape of the crystals against the bright green Bodipy 493/503 nm fluorescence of the immersion liquid. The right panels show the red TR fluorescence of the labeled protein.

was shown, that analyte spectra can be obtained from such preparations, even though the analyte is only chemisorbed at the matrix crystal surfaces [31]. However, the desorption is much less "soft" than MALDI-MS from samples with incorporated analytes, leading to a strongly increased metastable fragmentation of the ions and an upper mass limit for proteins of 30–55 kDa.

1.3 Absorption of the Laser Radiation

The role of the optical absorption of the matrix in the transfer of energy from the laser beam to the sample is governed by Beer's law, as described previously in 1985 [14].

$$H = H_0 * e^{-\alpha z} \tag{1.1}$$

where H is the laser fluence at depth z into the sample, H_0 is the laser fluence at the sample surface, and α is the absorption coefficient (see Chapter 2, Section 2.1 for a definition of the fluence). The absorption coefficient α equals the product of the molar absorption coefficient α_n and the concentration c_n of the absorbing molecules in the sample. The wavelength-dependent molar absorption coefficient α_n is a property of the matrix compound and, for UV-MALDI, has a maximum value of typically between 5×10^3 and 5×10^4 l mol^{-1} cm^{-1} at the peak absorption

wavelength. Molar absorption coefficients of this order of magnitude are only provided by molecules with aromatic rings; the exact wavelength of maximum absorption and its magnitude are determined by the ligands of the core ring and are tabulated in a variety of reference sources. Some care should be exercised in using the tabulated values for α_n, because they have all been measured for dilute solutions of the compounds. In the solid state of a typical MALDI sample the absorption bands are typically broadened and slightly red-shifted [32]. The concentration c_n of absorbers (chromophores) is unusually high in MALDI samples, about $10\,\mathrm{mol}\cdot\mathrm{l}^{-1}$, because all the solvent is evaporated before the sample is introduced into the vacuum. As a result, the absorption coefficient α ranges from about 5×10^4 to $5 \times 10^5\,\mathrm{cm}^{-1}$. The inverse of α is called the penetration depth δ, and has values of only 20 to 200 nm. It is the depth into the sample, at which the fluence has decreased to about 30% of the value at the surface. It is also an order of magnitude estimate of the depth of material ablated (desorbed) per single laser pulse in MALDI. Because of this very shallow ablation depth, a given location of the sample can usually be irradiated many times before the material is exhausted. For the MALDI process the "density" of energy, absorbed per unit volume E_a/V of the sample is the process-determining quantity. This can be derived from Eq. (1.1) by simple differentiation to:

$$E_a/V = \alpha * H \tag{1.2}$$

Equation 1.2 is at the core of the MALDI process. If a matrix is chosen with a sufficiently high absorption coefficient α, a relatively low fluence H_0 can be applied. Values for H_0 of 20–200 $\mathrm{J\,m^{-2}}$ are representative for most UV-MALDI applications. As discussed in Section 2.1, pulsed lasers with a pulse width of a few nanoseconds are employed in UV-MALDI. At a fluence of $100\,\mathrm{J\,m^{-2}}$ and a pulse width of 2 ns, the "intensity" (irradiance) of the laser beam at the sample surface is only $10^{11}\,\mathrm{W\,m^{-2}}$ or $10^7\,\mathrm{W\,cm^{-2}}$, not enough to induce any non-linear absorption such as non-resonant two-photon absorption. For the linear absorption the absorbed energy per unit volume can be controlled meticulously with a suitable variable attenuator in the laser beam, a feature which has turned out to be crucial for the successful MALDI of large molecules, because the desorption of non-volatile, labile molecules can only be achieved in a narrow range of energy "density". The other essential feature of this laser absorption is that the energy is transferred more or less uniformly to a macroscopic sample volume (except for the attenuation of the fluence into the sample and the fluence profile, as discussed in Section 2.1). This is very different from the situation in SIMS or PD, where incident particles create minute tracks of atomic dimensions of very high energy density in the sample, with a strong radial decline of energy density. This strongly heterogeneous energy distribution is the main reason for the limitation of these methods for the desorption of larger molecules. The fluence can also be converted into a value for the photon flux – that is, the number of photons impinging on the sample per single laser pulse. A fluence of $100\,\mathrm{J\,m^{-2}}$ corresponds to a photon flux of 1.7×10^{16} photons per cm^2; each carrying an energy of 3.7 eV at the wavelength of

337 nm of the N_2 laser. A molar absorption coefficient of $10^4\,l\,mol^{-1}\,cm^{-1}$ represents a physical absorption cross-section of the chromophore of $1.6 \times 10^{-17}\,cm^2$, resulting in an average of 0.7 photons absorbed per matrix molecule for any given laser exposure. This is, on the one hand, a very high density of excitation energy, close to the solid-state energy stored in all of the intermolecular bonds. It is, therefore not surprising that it leads to an explosive ablation of the excited sample volume. On the other hand, it renders even resonant two-photon absorption by the matrix rather unlikely. The high density of excited molecules does, however, result in a rather high rate of energy pooling in the sample, in which two neighboring excited molecules pool their energy, with one of them acquiring twice the photon energy and the other falling back to the ground state [33]. This energy pooling is an important feature in some models for the ionization of the molecules which requires at least the energy of two photons for an initial photoionization of the matrix molecules [34]. The situation is similar, but not equal, for IR-MALDI. Optical absorption in the infrared region of the spectrum represents a transition between vibrational or rotational molecular states. These transitions are typically weaker than the electronic transitions in the UV by one to two orders of magnitude. The strongest such transitions are those of the O–H and N–H stretch vibrations near a 3 μm wavelength. The absorption coefficient not only of water or vacuum-stable ice, but also of the common IR-MALDI matrix glycerol, in this wavelength region reaches peak values of $10^4\,cm^{-1}$, corresponding to a penetration depth of about 1 μm – more than 20-fold that of typical penetration depths in the UV. As a result, the ablated mass per laser exposure in IR-MALDI exceeds that of UV-MALDI by at least a factor of 10, and the sample consumption rate is accordingly higher. Typical laser fluences for IR-MALDI range from 10^3 to $5 \times 10^3\,J\,m^{-2}$. Non-linear absorption processes are even less likely for such fluences in the infrared as compared to UV-MALDI, and for the photon energy of only 0.3 eV or less even the absorption of several photons by a given chromophore or energy pooling cannot possibly excite single molecules to anywhere near their ionization energy.

1.4 The Ablation/Desorption Process

As discussed above, every laser exposure of a sample leads to the removal of a bulk volume – that is, many monolayers of matrix molecules of the sample. The term "desorption" is, therefore, somewhat ill-chosen for this process, and was so even for the field desorption for which it was originally coined. Ablation is the more correct term, and this is used interchangeably with desorption throughout this chapter. The processes of material ablation and the ionization of a minor fraction of the matrix and analyte molecules are, no doubt, intimately intertwined, and both take place on a micrometer geometrical and a nanosecond time scale. It is experimentally very difficult – if not impossible – to sort out the complex contributions of the physical processes induced by the laser irradiation in all detail. Despite this complexity, it is of considerable merit to treat the two mechanisms separately, and

some basic understanding can be derived from such a discussion, this particularly, because the vast majority of material comes off as neutrals.

As was pointed out above, even at the threshold fluence for the detection of MALDI ions each laser pulse transfers an amount of energy to the sample, close to the sum of all bond energies in the solid (equivalent to the sum of the heat of fusion and evaporation). Even though this energy will in all cases lead to ablation of the excited volume, different energy dissipation processes need to be taken into account. Energy dissipation by heat conduction during the laser pulse can be neglected in all cases of UV- as well as IR-MALDI. For a penetration depth of laser radiation of 100 nm, the time constant for heat conduction of typical UV-MALDI matrices is about 10 ns – still a factor of three longer than the typical laser pulse width. In the infrared, the heat conduction time constant for 1 μm penetration depth is about 1 μs, a factor of about 10 longer than the longest pulse width of lasers (Er:YAG) used in that case. The very rapid heating of the sample by the laser radiation will also generate a thermoelastic pressure pulse in the absorbing sample volume which travels out of the excited volume with the speed of sound, carrying away part of the deposited energy. With a speed of sound in typical crystalline matrices of 2000–3000 ms^{-1} and depth of 100 nm in the UV, the acoustic time constant is less than 100 ps, much shorter than the laser pulse width of a few nanoseconds. Even though energy is constantly carried away by the pressure wave, this amounts only to a very small fraction of the total deposited energy, and the pressure in the excited volume never reaches values high enough to substantially influence the ablation process. For IR-MALDI, the situation can be very different because of the larger penetration depth. For the desorption with an Er:YAG laser the pulse width of 100 ns is long compared to the acoustic time constant, with only a negligible pressure build-up in the excited volume. The pulse width of the optical parametric oscillator (OPO) laser of only 6 ns, however, is rather close to the acoustic time constant, and the system stays close to what is called the "acoustic confinement". In this case a very high pressure of several tens of MegaPascal can build up in the excited volume. Rohlfing et al. [35] have investigated the ablation processes by measuring the recoil pressure of the ablated material with a fast acoustic transducer onto which the sample was prepared, while Leisner et al. [36] have studied the expanding plume of ablated material with high-speed time-lapse photography, both at a wavelength of 2.94 μm. Both measurements were much easier for IR-MALDI and glycerol as a matrix, because of the higher amount of material ablated. For the short pulse width and near-acoustic confinement, these authors saw pressure pulses of very high amplitude as expected, and time durations comparable to the laser pulse. For the 100-ns pulses of the Er:YAG laser, the pressure amplitude was low, but lasted for several microseconds. The plume photographs revealed that material is removed from the sample for times of up to over 100 μs in both cases. This is certainly somewhat of a surprise, because the TOF analysis had revealed that the ions are only generated during an initial phase of not longer than about 300 ns [37]. Similar experiments were conducted by Rohlfing under UV-MALDI conditions [38], using the liquid matrix nitrobenzylalcohol for better sample homogeneity and a desorption wavelength of 266 nm.

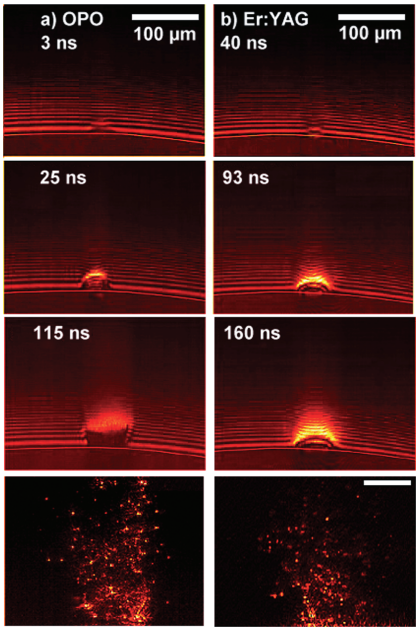

Fig. 1.2 High-speed time-lapse photographs of IR-MALDI plumes generated with an optical parametric oscillator (OPO) laser with 6-ns pulse width and an Er:Yag-laser with 100-ns pulse width. Both lasers were operated at 2.94 µm wavelength. Matrix: glycerol; time resolution 8 ns; spatial resolution 4 µm. The top three panels represent gradients of gaseous material density creating gradients of the index of refraction in the plume, recorded in a dark-field illumination mode. The lowest panel represents particle emission in the plume recorded with light scattered at 90° to the illumination beam. The thin lowest line indicates the top surface of the glycerol drop; the other striations in the dark-field images are artifacts of optical interference.

Expectedly, the recoil pressure was very low – lower even than that of the long-pulse IR-laser – because of the smaller amount of removed material. The recoil pressure pulse lasted for only less than 25 ns, the time resolution of the detection. The plume photographs revealed a material ejection for up to at least several microseconds, again much longer than the ion generation time of at most a few nanoseconds. Some typical plume photographs are shown in Figures 1.2 and 1.3. The results of these experiment can tentatively be explained by the following models. In IR-MALDI with 100 ns-long ER:YAG-laser pulses, the absorbing volume is superheated to a temperature that is substantially above the boiling temperature, followed by a volume ejection of material through boiling by heterogeneous nucleation. The situation is similar for UV-MALDI. The longer time course of material ejection in the infrared as compared to the UV is caused by a deeper penetration of the radiation into the sample, and a correspondingly higher inertia and residual heat of the excited volume. For the 6-ns pulses in IR-MALDI of the OPO-laser, the ablation process is substantially different. The strong thermoelastic wave is reflected at the sample vacuum interface, thereby reversing its phase.

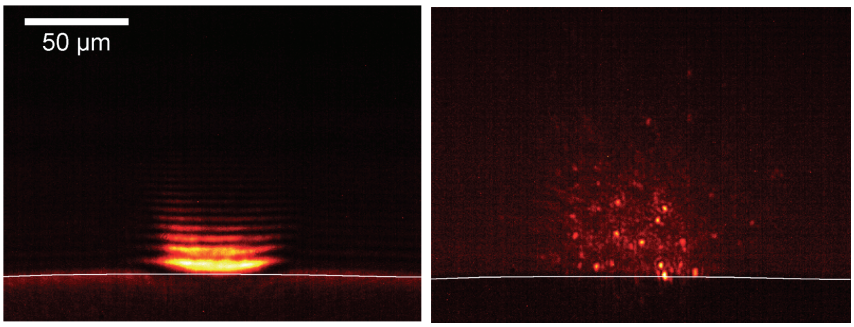

Fig. 1.3 High-speed photographs of UV-MALDI plumes generated with a frequency-quadrupled Nd:YAG laser of 266 nm wavelength and 8 ns pulse width. Matrix: nitrobenzylalcohol; time resolution 8 ns; spatial resolution 4 µm. Left panel: dark-field image, 45 ns after laser exposure. Right panel: 90° scattered light image, 311 ns after exposure. The thin lowest line indicates the top surface of the glycerol drop; the other striations in the dark-field image are artifacts of optical interference.

It then travels back into the sample as a tensile wave, transferring the material beyond the liquid spinodal, as described by Vogel and Venugopalan for soft-tissue ablation [39]. Upon this transition, the material goes through a phase explosion by homogeneous nucleation. Even though all of these experiments were conducted on liquid samples to keep reproducibility high, they reflect, most probably, also the situation for crystalline solid samples. A contribution by the gaseous components such as CO_2 through thermal decomposition of matrix molecules is also discussed as a source of pressure build-up in the excited volume.

Theoretical models for the ionization as well as molecular modeling suggest that the ablation process generates clusters and material particles besides gaseous components. Particles are indeed seen in the plume photographs, though only at times late during the ablation, when the generation of ions is long over. Thus, this particle emission does not seem to be relevant for the MALDI ion generation. During the early expansion phase of the plume, dark-field images reveal homogeneous gradients of the index of refraction. However, the spatial resolution of the plume photographs is only a few micrometers; a distribution of clusters of different size, expected during the early phase of the plume expansion, is, therefore, not excluded by the experimental observations.

Garrison, Zhigilei [40,41] and co-workers as well as Knochenmuss [34] have modeled the ablation process using molecular dynamics simulation. Qualitatively, these simulations correctly predict many of the features observed experimentally. Particularly interesting is the consistent prediction that, while clusters are formed early during the ablation process, their internal energy does not seem to suffice for a decay by matrix evaporation, one of the assumptions of the "lucky survivor" model for ionization (see Section 1.5). It must also be observed that these simulations contain significant simplifications and, most probably more restrictive, must be scaled to very small volumes and short time regimes because of limited computation capacity. These models have become significantly refined

over the past few years and will, no doubt, continue to do so. In this respect they will clearly contribute to our understanding of MALDI processes in the future.

1.5 Ionization

The mechanisms which lead to the formation of charged matrix and analyte molecules in the MALDI process are even more poorly understood than the physics of the material ablation/desorption. For a better understanding, it is important to distinguish between the ionization of matrix molecules and that of the analytes. Although no precise numbers have been determined experimentally, it is, most probably, safe to assume that the ion yield for the matrix (i.e., the ratio of ions to neutrals) is somewhere in the range of 10^{-5} to 10^{-3}. The ion yield of the analytes can be much higher, in the order of 0.1–1% for typical cases, and above 10% in exceptional cases. The intensity of the ion signals, as determined from the spectra, are not independent of each other, because charge transfer processes between the two species are, in all likelihood, taking place in the expanding plume and possibly already in the solid state upon laser irradiation. In favorable cases, the spectra even show intense analyte ion signals with negligible matrix ions, despite a typical 10^4 excess of the matrix [42].

Two models for ion formation have been proposed. The older model assumes neutral analyte molecules in the matrix crystals and a photoionization of the matrix molecules as the initial step [43,44], followed by charge transfer to the analyte molecules in the plume. The more recent "lucky survivor" model [45] assumes that proteins are incorporated into the matrix as charged species, most of which become re-neutralized within desorbed clusters of matrix and analyte.

For a laser wavelength of 337 or 355 nm (i.e., photon energies of 3.6 and 3.3 eV, respectively), at least two photons are needed for a photoionization of matrix molecules. The typical MALDI laser photon fluxes are too low for any significant resonant two-photon absorption to take place, but very efficient energy pooling between excited neighboring molecules in the crystals has been demonstrated [33]. In the gas phase, even the energy of two photons does not suffice for ionization, but in the solid phase of the crystals the ionization potential may be somewhat lower, and/or thermal energy may make up for the difference. A reaction of the photoelectron with neutral matrix molecules will give rise to negative ions beside the positive ones [44]. The frequent observation of radical matrix ions such as $M^{+\cdot}$ and/or $[M+2H]^{+\cdot}$ and a $[M-2H]^{-\cdot}$ ion besides the expected even-electron ions, among them $[M+H]^+$- or $[M-H]^-$- as well as a prominent $[2M+H-2H_2O]^+$ for 2,5-DHB and $[2MH]^+$- for CHCA is at least in agreement with the photoionization model, if not a strong indication (Fig. 1.4). As for the model prediction of the relative yield of positive versus negative analyte ions of peptides/proteins, it must be considered that the protonated matrix molecules with proton affinities between 180 and 215 kcal mol^{-1} [46] are strong gas-phase acids in comparison to basic amino acids with a much higher proton affinity (up to 245 kcal mol^{-1} for arginine) [47], result-

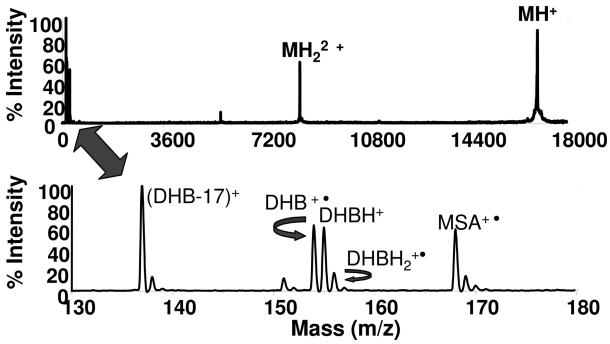

Fig. 1.4 UV-MALDI mass spectrum of myoglobin. Matrix: DHBs (2,5-dihydroxybenzoic acid (DHB) plus 2-hydroxy-5-methoxysalicylic acid (MSA); 9:1). Wavelength, 337 nm; Mass analyzer, Reflectron TOF.

ing in an efficient charge transfer and formation of positively charged analyte ions. In contrast, no such difference in basicity between negatively charged ions of matrix and peptides exists, because both are typically carboxylate anions with very close proton affinities; this should limit the yield of analyte anions.

Recently, Knochenmuss has developed a quantitative model based on the matrix photoionization model [48,49]. One argument against this model is the observation that MALDI spectra, obtained with infrared lasers at a 1.94 μm wavelength, closely resemble the UV-MALDI spectra, including radical matrix ions observed (e.g., for the succinic acid matrix). The photon energy of only 0.4 eV at this wavelength certainly excludes photoionization. Similarity of the spectra alone does, however, not suffice as proof of identical ionization processes at the two wavelengths, and indeed the ion yield for analytes in the infrared is about an order of magnitude lower than in the UV.

The more recent "lucky survivor" model of Karas et al. proposes that proteins retain their solution charge state upon incorporation into the matrix. This assumption is based on the observation that pH-indicator molecules retain their color and charge state upon crystal incorporation for acidic, neutral, or basic matrices [28]. For most common acidic matrices, almost all peptides will carry a (multiple) positive excess charge; counterions will then typically be either trifluoroacetate or matrix anions. In order to maintain the positive charges of the peptides and to keep the negative counterions separate, the analytes must be incorporated at least in a partially solvated form. In a second step, the model assumes a break-up of the crystal lattice into small clusters upon desorption, some of them with only a single analyte ion. Statistically, some of these clusters are assumed to carry a positive or negative charge by deficit, or an excess of a single counterion. In the expanding plume the clusters are assumed to lose neutral matrix and solvent molecules as well as counterions as free acids or bases after

their proton-transfer neutralization with analyte (de)protonation sites. This results in a neutralization of the peptide charges except for the only remaining excess charge:

$$(1a)\quad \{(M + nH)^{n+} + (n - 1)A^-\}^{1+} \rightarrow [M + H]^+ + (n - 1)HA$$

$$(1b)\quad \{(M - nH)^{n-} + (n - 1)BH^+\}^{1-} \rightarrow [M - H]^- + (n - 1)B$$

These singly charged analyte ions are the lucky survivors of the neutralization process. The model elegantly explains the observation of mostly singly charged ions in MALDI spectra, and would work equally well for UV- as well as IR-MALDI. The formation of matrix/analyte clusters in the desorption process is also predicted by molecular modeling [40,41]. However, these model calculations also predict that the clusters have not enough internal energy for the proposed evaporation of the neutrals.

One of the strengths of the lucky-survivor model is that it can be equally well applied to account for the formation of negative ions from acidic conditions (2a), or the formation of positively charged ions of polyanionic (in solution) species such as nucleic acids (2b) with matrices such as 3-hydroxypicolinic acid or the trihydroxyacetophenones.

$$(2a)\quad \{[M + nH]^{n+} + (n + 1)A^-\}^- \rightarrow [M + A]^- + nHA \rightarrow [M - H]^- + (n + 1)HA$$

$$(2b)\quad \{(M - nH)^{n-} + (n + 1)BH^+\}^+ \rightarrow [M + BH]^+ + nB \rightarrow [MH]^+ + (n + 1)B$$

with {} as a symbol for the intermediate cluster, A^- and HA for the anion and respective conjugate acid (such as TFA^-/HTFA) and B and BH^+ for a base and its conjugate acid (such as NH_3/NH^{4+}).

While these ionic cluster ions {. . . . .} never show up in the MALDI spectra with the typical solutes used (e.g., trifluoroacetic acid (TFA) or ammonium salts), they have been detected for extremely strong acids [50]; their conjugate anions are extremely weak bases and thus stabilize the formed ion pairs with protonated analyte sites. Even though the relative abundance of positive to negative ions of a given analyte under typical MALDI conditions seems never to have been carefully determined, the postulate of an intermediate anion adduct $[M + A]^-$ in (2a) rationalizes the general observation that the formation of negative peptide ions out of typically acidic matrix solution is substantially less effective, because the proton-transfer step necessary to form the $[M\text{-}H]^-$-ion competes with the simple dissociation of the adduct ion. Similar arguments hold for the polyanionic nucleic acids. Whilst the addition of ammonium ions result in a quantitative detection of the free acids, a substitution of the ammonium by alkyl-quaternary ammonium ions leads to the observation of adduct ions, increasing in intensity with increasing length of the alkyl chains.

Besides the processes suggested for the lucky survivor model, matrix photoionization is also probable as a parallel process, as documented by the observed

matrix ions. In UV-MALDI, both processes may therefore contribute to the observed analyte ions to an as-yet unknown degree.

For analytes of very low proton affinity such as neutral carbohydrates and many synthetic polymers, cationization by Na^+, K^+ or other metal cations is usually observed in MALDI (see Chapters 6, 7 and 8). The cationization in all likelihood takes place in the expanding plume. It requires a co-desorption of the analyte, and the cations and best results are therefore obtained from sample locations where both species exist in close neighborhood, such as in the center of DHB-dried droplet preparations. Specific protocols have been developed for the MALDI of such analytes [51].

1.6 Fragmentation of MALDI Ions

Fragmentation of MALDI ions is a mixed blessing, as in all of MS. It can, on the one hand, lead to a substantial loss of spectra quality such as loss of mass resolution or even complete loss of the signal of the intact parent ion, as has been shown for the loss of sialic acids in the analysis of glycoconjugates in reflectron-TOF analyzers [52]. On the other hand, intrinsic or induced fragmentation is an indispensable tool for the acquisition of structural information in MS^n experiments. The nomenclature for the fragmentation – particularly the differentiation in post-source-decay (PSD) and in-source-decay ions – is closely related to time-of-flight analyzers, because they still constitute the majority of spectrometers used for the analysis of MALDI ions. The details of how to analyze fragment ions with different types of instrument are discussed in Chapter 2 (see Section 2.4.3 in particular).

Even though some limited ion stability – and thus fragmentation – was obvious in the early days of MALDI by peak tailing on the low mass side, and was attributed to small neutral losses of peptide and protein ions, the fact that MALDI can generate substantial prompt and metastable fragmentation of analyte ions was obscured at an early stage. This was due to two facts: the laser microprobe instrument (LAMMA 1000) used for the initial experiments indeed minimized fragmentation because of a very week acceleration field strength and low total (3 keV) ion energy; the next-generation MALDI-TOF instruments were linear instruments in which metastable fragment ions cannot be observed directly.

It was only when Kaufmann and Spengler started careful investigations of ion stability using a deceleration stage in a linear TOF instrument that the potentially high degree of metastable fragmentation was detected [53]. This was the starting point for the development of the so-called PSD analysis of metastable ions which led to today's MALDI-TOF/TOF instruments [54–56]. The character of the PSD fragmentation – that is, the classes of fragment ions observed – is in full agreement with a collisional activation process. Despite this general

agreement, PSD mass spectra are often more complex than CID mass spectra, showing internal fragments and products of consecutive fragmentations, and pointing to more complex excitation mechanisms of the intramolecular degrees of freedom. Besides collisional excitation through collisions of the ions with neutrals in the plume, a direct excitation in the matrix crystal after absorption of the laser energy and excess energy of chemical reactions in the plume such as proton transfer must be considered. All of these processes depend in complex fashion on instrumental parameters such as laser fluence and focus, ion extraction field strength and delay, as well as on the choice of matrix. Information about the different contributions to ion excitation have been listed in a report which compares vacuum MALDI to atmospheric-pressure MALDI [57]; this report provides a comprehensive summary of the current knowledge of MALDI fragmentation. The effect of collisional excitation upon acceleration was demonstrated for matrix ions. These AP-MALDI investigations were later extended to determine initial MALDI plume excitation processes [58], including the application to more representative test samples than thermometer molecules, such as a model peptide and a nucleoside. Here, matrix softness yielded the best agreement with matrix proton affinity. In general, matrix proton affinities have been used with only limited success to rank matrices with respect to their effectiveness for fragmentation. In a practical approach, matrices are classified and ranked from "hard" to "soft". α-cyano-4-hydroxycinnamic acid, the matrix preferentially applied for "peptide-mass fingerprint" analyses in proteomics because of its rather homogeneous sample morphology, is one of the hardest matrices in that ranking. Because of its degree of fragmentation induction, it is also the matrix of choice for PSD- or TOF/TOF-experiments. "Super DHB" (DHBs; 2,5-DHB with a 5–10% addition of 2-hydroxy-5-methoxybenzoic acid) is on the soft end of the list and, therefore, preferentially applied for the analysis of larger proteins. By using such a soft matrix and optimizing all instrumental parameters (low extraction field, long delay times), small-neutral loss can be minimized and a good mass resolution (close to the theoretical limit) is obtainable for a linear TOF configuration, even for medium size proteins up to bovine serum albumin [59]. Common for PSD and the low-energy CID mechanisms is the randomization of the internal energy among all internal degrees of freedom before the (metastable) fragmentation. Interestingly, it was found that the order of matrices from hard to soft agrees with the initial ion velocities determined in a linear TOF. Hard matrices correlate with low initial velocities, and vice versa [60]. This points to a role for expansion cooling in the MALDI desorption process.

A very different fragmentation mechanism was first reported by R.S. Brown et al. [61,62], whereby fragment ions are formed "promptly" upon ion generation/excitation with a time delay of less than at most 100 ns – substantially less than the typical delay times in delayed-extraction TOF instruments. Therefore, these are referred to as in-source-decay (ISD) ions. ISD spectra contain signals of c- and sometimes z-type fragment ions, in addition to some a-, b- and y-ions (for fragment ion nomenclature, see Chapter 3). This type of fragmentation is observed

for both positive and negative ions, indicating that ISD is independent of proton transfer, and 2,5-DHB is the matrix with the highest ISD yields [63–65]. The analogy to electron capture dissociation prompted a discussion on the possible role of electrons in ISD, although it appears clear today that ISD is mediated by hydrogen radicals [66]. ISD yields a substantially more complete fragment-ion series as compared to PSD, although hopes to use it for practical applications (e.g., in proteomics [67,68]) have not materialized, mostly because of the low intensity of the signals. An additional problem is that true MS/MS experiments cannot be carried out as a precursor selection for peptides from a mixture is not possible.

1.7 MALDI of Non-Covalent Complexes

After about 20 years' use of MALDI-MS, it is clear that the successful analysis of non-covalent interactions and complexes is rather the exception than the rule. Considering most typical MALDI protocols, this cannot be a surprise. Most "classical" matrices are organic acids and typically used in water/organic solvent mixtures, often acidified by TFA, i.e., in conditions which should result in the dissociation of most (if not all) non-covalent complexes. However, signals of non-covalent complexes have indeed been obtained from such preparations [69,70]. At least for some such systems, the dissociation seems to be sufficiently slow that a fast evaporation of the solvent conserves at least a certain fraction of the complexes. Unfortunately, adjustment of the pH and the omission of organic solvent is often not a viable alternative, as acidic matrices will be deprotonated and totally change their crystallization and incorporation properties as salts. Many salts and buffers used to adjust ionic strength/pH are, therefore, not MALDI-compatible in the desired concentration, or at least compromise the performance with respect to sensitivity and mass resolution.

The incorporation of analytes into the matrix crystals, which has been shown generally to make the desorption process softer or altogether possible [31], is another step which might lead to dissociation of the complexes. This question has been addressed in order to understand the so-called "first-shot phenomenon", which had been observed much earlier but only recently had been resolved [71,72]. For a number of selected matrices, the signals of protein–protein complexes are observed only in the spectra of first exposures of a given sample spot. Subsequent exposures yield only signals of the monomer units. By a combination of MALDI-MS and confocal laser scanning microscopy (CLSM) of complexes with fluorochromes, which exhibit a fluorescence resonance energy transfer (FRET), it was shown that in these systems the complexes dissociate upon incorporation, whereas intact complexes are precipitated at the surface of matrix crystals. The next crucial step is the intact desorption and ionization of the complex and their survival in the gas phase of the expanding plume. Such dissociation upon desorption is even more likely if the complexes are localized at the crystal surface rather than being incorporated.

The type of interaction within the complex is also a decisive parameter. From energetic considerations it is obvious that gas-phase stability of non-covalent complexes is highest for ionic interactions, followed by hydrogen bonding. Interestingly, the formation of strong ionic complexes has even been used to facilitate MALDI measurement of highly acidic and thus negatively charged biocompounds, such as oligonucleotides and heparin-derived oligosaccharides, by admixing highly basic peptides, followed by a mass determination of the intact stable complex [73]. Hydrophobic interaction should be particularly labile, because it is based on the hydrophilic environment of the solvent water, lost in the vacuum. The simple detection of non-covalent complexes by ESI shows, that the transfer of the molecule into the vacuum does not necessarily result in a dissociation, if the internal energy does not suffice for the transition to the very different conformational state. It would also appear that complexes with large contact areas between the constituents of the complex and corresponding contribution of salt- and hydrogen bridges, as well as hydrophobic interaction typical of many protein–protein complexes help to stabilize the complex. Complexes between small and large molecules, as are typical for ligand–receptor or antigen–antibody systems, are much more difficult to analyze by MALDI-MS. Their affinity depend on the exact conservation of the conformation in small epitopes of the protein, which is more easily lost in the MALDI process than the complete quaternary structure. Interestingly, spectra of the intact biotin–streptavidin complex, one of the strongest complexes known to date, have never been obtained by MALDI.

Another issue which complicates the use of MALDI for the analysis of non-covalent complexes is the formation of non-specific multimeric and adduct ions. This effect is even more pronounced for the analysis of non-covalent protein complexes, as high concentrations (10 pmol μl^{-1} or higher) of analyte are typically used to overcome the reduced sensitivity of TOF instruments in the high mass range. Furthermore an elevated laser fluence, as well as deviation from optimal preparation protocols, are aggravating effects. It is, therefore, most important clearly to differentiate specific from non-specific interactions, and this is typically achieved by using a known non-binding/non-interacting control compound. Because of these limitations, analyses of non-covalent interactions by MALDI are typically qualitative rather than quantitative.

Within these boundary conditions, a number of reports have described the successful detection of several types of non-covalent complex [74–81]. During the early days of MALDI, high-intensity signals of non-covalent protein complexes using a nicotinic acid matrix and a laser wavelength of 266 nm were reported, for example of the tetrameric glucose isomerase [82] and a trimeric porin [83]. Comprehensive reviews have been provided by Hillenkamp [84] and Farmer and Caprioli [85] on this subject. In addition, a recent report by Zehl and Allmaier on the influence of instrumental parameters for the detection of quaternary protein structures starts from a careful review of the state of the art [86], and provides a critical discussion on the above-described problems. These authors used 2,6-dihydroxyacetophenone as (non-acidic) matrix with the addition of ammonium acetate or diammonium citrate (DAHC) to adjust solution conditions for the

stabilization of protein complexes. Another only slightly acidic matrix which tolerates even high additive amounts such as DAHC is 6-azathiothymine (ATT); this was also used to investigate nucleic acids and their non-covalent complexes and adducts [87]. Superior results for double-stranded DNA were, however, obtained when using glycerol as a matrix for IR-MALDI [88].

In summary, the use of MALDI to investigate non-covalent interaction is far less straightforward than typical applications for peptides and proteins under denaturing conditions. Success is not predictable, and careful control experiments must be implemented to differentiate specific from non-specific interactions. It appears, however, that the potential of MALDI in this area is far from being fully explored. Recently, a new approach was presented investigating the formation of non-covalent complexes, based on the detection of the "intensity fading" of one complex partner [89,90], rather than of the intact complex. This approach avoids the problems related to detection of the intact complex in the high mass range, and can be carried out at analytically relevant micromolar and sub-micromolar concentration levels.

1.8 The Correct Choice of Matrix: Sample Preparation

Unfortunately or expectedly, there is no single MALDI matrix or sample preparation protocol which is suited to all analytical problems and analytes in MALDI-MS. A few of the more general considerations are discussed in the following section, though more specific information is provided in the applications chapters of this book. A representative list of commonly used matrices and their main properties is provided in Table 1.1. There are different matrices of first choice for different classes of analytes and analytical problems. For example, CHCA is used in the majority of proteomics applications for the analysis of peptide-mass-fingerprints generated by protein enzymatic digests (as discussed later). On the other hand, 2,5-DHB – and especially DHBs (i.e., DHB with an admixture of 5–10% 5-methoxy-2-hydroxybenzoic acid) – with its pronounced crystallization into large crystals of ca. 100 μm size is particularly suited to protein analysis. The reasons for this are, first, because its softness prevents strong small-neutral losses and peak tailing; and second, because the crystals incorporate the proteins, but exclude the majority of common contaminants.

A practical overview of the various matrices and preparation techniques can be found, for example, on the Internet at: http://www.chemistry.wustl.edu/~msf/damon/sample_prep_toc.html, as well as on the Internet pages of commercial suppliers of chemicals.

The "dried droplet" standard MALDI sample preparation is very simple. Here, the sample and matrix are dissolved in a common solvent or solvent system, and mixed either before deposition onto or directly on the MALDI sample support. The matrix-analyte droplet of typically 1 μL volume is then slowly dried in air, or under a forced flow of cold air. This results in a deposit of crystals which, de-

Table 1.1 A selection of commonly used MALDI matrices.

Matrix	*Structure*	*Wavelength*	*Major applications*
Nicotinic acid	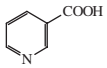	UV 266 nm	Proteins, peptides, adduct formation
2,5-Dihydroxybenzoic acid (plus 10% 2-hydroxy-5-methoxybenzoic acid)	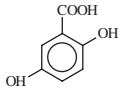	UV 337 nm, 353 nm	Proteins, peptides, carbohydrates, synthetic polymers
Sinapinic acid	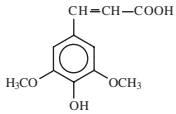	UV 337 nm, 353 nm	Proteins, peptides
α-Cyano-4-hydroxycinnamic acid	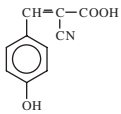	UV 337 nm, 353 nm	Peptides, fragmentation
3-Hydroxy-picolinic acid	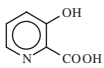	UV 337 nm, 353 nm	Best for nucleic acids
6-Aza-2-thiothymine	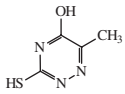	UV 337 nm, 353 nm	Proteins, peptides, non-covalent complexes; near-neutral pH
k,m,n-Di(tri)hydroxy-acetophenone	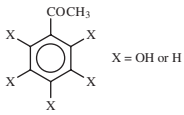	UV 337 nm, 353 nm	Protein, peptides, non-covalent complexes; near-neutral pH
Succinic acid	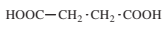	IR 2.94 μm, 2.79 μm	Proteins, peptides
Glycerol	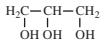	IR 2.94 μm, 2.79 μm	Proteins, peptides, liquid matrix

IR = infrared; UV = ultraviolet.

pending on the matrix, vary between submicrometer and several hundred micrometers in size. In many cases, surface tension leads to a non-homogeneous distribution of the individual crystals near the rim of the preparation. The best MALDI performance is usually achieved only at certain locations of the crystals, which often requires manual interference and active control by the experimenter; this is why most MALDI instruments are equipped with a microscopic observation system. The cause of these "sweet spots" has been the subject of much speculation, the commonly held notion being that of an inhomogeneous distribution of analyte within the crystals. However, this has been disproved by Horneffer et al., who found a homogeneous distribution of fluorescently labeled analyte in the crystals of a representative number of different matrix crystals by CLSM

studies (see Section 1.2). A different (ionization) state of the analyte molecules in different locations, or heterogeneous orientation of the matrix crystal surfaces relative to the spectrometer axis and perpendicular to which the ions are ejected in conjunction with the limited angular acceptance of the mass spectrometer, might also cause the observed sweet spots.

As a rule of thumb, the addition of the analyte solution should not noticeably change the crystallization behavior of the neat matrix; this already indicates that the solution excess of the matrix with respect to the analyte is maintained in the crystals, and that the contaminant level is low enough. Any solute component which dramatically changes the appearance of the matrix crystals or prevents crystallization altogether – for example, low-volatility solvents such as glycerol or dimethyl sulfoxide – will prohibit a successful MALDI analysis.

Over the years, a large number of modifications of, or alternatives to, the dried-droplet technique have been developed. These many variations are often the personal preferences of MALDI users for sample preparation, and the subject may appear to be an art or a even a "black art". However, dried-droplet protocols are still the most widely used with high success. It also appears that instrumental developments using lasers with higher frequencies, together with the automation of the entire MALDI measurements, have eased the problems of heterogeneity to some extent. Among the many modifications and variations of the simple dried droplet preparation, two alternatives stand out as particularly useful and widespread, namely "surface preparation" and "anchor sample plates".

1.8.1 Surface Preparation

Surface preparation or predeposited matrix crystal layers were also often called thin layer preparation introduced to enhance sensitivity, homogeneity of the preparation, automation, and liquid chromatography (LC)-spotting.

Surface preparation was a true innovation [91]. It was shown that for the CHCA matrix, rapid evaporation of the organic solvent generates a relatively homogeneous, microcrystalline seed layer. Upon addition of the aqueous peptide analyte solution, only the very top layers of the nearly water-insoluble matrix redissolve and incorporate the analyte. The concentration of the whole analyte into only a limited depth layer at the radiation-accessible top of the preparation results in an improved sensitivity, and the structurally relatively homogeneous crystal layer improves the mass resolution, particularly in linear TOF mass spectrometers. Unfortunately, this approach is restricted to matrices which do not fully dissolve in the usually aqueous analyte solvent. However, it is generally believed that, despite its limited solubility, the matrix is partially dissolved by the analyte solution and that true incorporation of the analyte into the matrix takes place. It was, moreover, shown that contaminants such as salts could be rinsed from the surface with a splash of ice water, without any major loss in sensitivity. Hence, surface preparation became the starting point for the development of disposable MALDI targets with predeposited matrix spots. The generation of more homogeneous micro-

crystalline sample layers by rapid evaporation of the solvent (e.g., *in vacuo*) has also been used for a variety of other matrices.

1.8.2 Anchor Sample Plates

Anchor plates for the preparation of multiple samples have small hydrophilic islands, typically of 100–500 μm diameter, placed on a hydrophobic surface [92]. The hydrophobic surface prevents spreading of the sample solution over a large area, as otherwise observed for dried-droplet preparations. Instead, before and/or during crystallization of the matrix, the solution contracts onto these islands, thereby concentrating the matrix and analyte into a defined volume. This up-concentration is particularly useful for low-concentration analyte and matrix solutions, and also facilitates automated analyses of the fixed location samples.

A few other modifications of the sample preparation have also proven useful in specific cases:

- Mixtures of several different matrices have been reported for an improved performance, but so far only DHBs (a mixture of 90–95% 2,5-DHB and 5–10% 2-hydroxy-5-methoxybenzoic acid) has found relatively widespread application for proteins [93]. It softens the desorption and limits the small neutral loss and thereby improves mass resolution. A mixture of different trihydroxyacetophenones is sometimes used for the analysis of nucleic acids [94].
- Additives to matrix preparations are mostly used for sample clean-up. These additives do not absorb the laser radiation, but may influence the crystallization behavior of the matrix to some extent. The most frequently used method is to add DAHC as a cation scavenger to preparations of highly anionic samples such as nucleic acids [95]. The addition of ammonium phosphate to improve peptide-mass-fingerprint mass spectra by suppression of matrix cation clusters, and the use of phosphoric acid to improve DHB analysis of phosphopeptides, are two recent successful examples of this approach [96–98].

Modified surfaces, for example of sample plates, can be used for the affinity capture of analytes from crude mixtures. These can significantly enhance detection sensitivity and can be used for a simple sample clean-up. Titania (TiO_2) -coated surfaces or sol-gel systems, for example, have been shown to very selectively concentrate phosphopeptides from peptide fingerprint samples [99,100].

SELDI ("surface-enhanced laser desorption ionization") uses so-called protein chips for the detection of peptides and proteins from complex biological fluids such as blood. These protein chips contain various chromatographic media immobilized on a MALDI sample plate for the selective enrichment of constituents

of the complex mixture applied. Unfortunately, a large number of unsubstantiated claims for the detection of disease-related biomarkers, mostly as a result of poor mass spectrometric performance, has discredited this approach.

Liquid matrices could avoid the undesirable heterogeneity of crystalline MALDI samples. Liquid matrices (e.g., nitrobenzylalcohol and nitrophenyloctlyether) were introduced in the early UV-MALDI reports, but never found widespread application because their performance proved to be significantly inferior to that of the solid matrices, particularly because of extensive adduct formation. A more recent development is the synthesis of ionic liquid matrices, which are synthesized by preparing a 1:1 solution of a classical organic acid matrix and an organic base [101]. A comprehensive review on the first five years of ionic-liquid matrices was recently published [102]. Unfortunately, the products with the best performance for MALDI are either solid or very highly viscous liquids. To date, these matrices seem to be mostly restricted to the MALDI-MS of small, stable analytes.

A solvent-free preparation is of particular interest for the analysis of synthetic polymers for which a common solvent with a suitable matrix is not available, and for which sizeable amounts of material are usually available [103]. In this protocol, the analyte and matrix are ground thoroughly in a mortar or ball-mill and loaded onto a MALDI target as powders, or after having been pressed into pellets. Good mass spectra can be obtained for analytes up to a mass of ca. 30 kDa, even though the analytes are not incorporated into the matrix crystals [31].

Abbreviations

CLSM	Confocal Laser Scan Microscopy
DAHC	Diammonium Citrate
DHB/2,5-DHB	(2,5-) dihydroxybenzioc acid
2,6-DHB	2,6-dihydroxybenzioc acid
DHBs	"super" DHB (mixture of 95% DHB and 5% 2-hydroxy-5-methoxy-benzoic acid
DIOS	Desorption/Ionzation On Silicon
ESI	Electrospray Ionization
FAB	Fast Atom Bombardment
FD	Field Desorption
FRET	Fluorescence Resonant Energy Transfer
HCCA	4-hydroxy-α-cyanocinnamic acid
ISD	In Source Decay
LAMMA	Laser Microprobe Mass Analyzer
MALDI	Matrix Assisted Laser Desorption/Ionization
UV-MALDI	MALDI with ultraviolet laser wavelengths
IR-MALDI	MALDI with infrared laser wavelengths
AP-MALDI	MALDI at Atmospheric Pressure
MS	Mass Spectrometry
PD	Plasma Desorption
PSD	Post Source Decay
SALDI	Surface Assisted Laser Desorption/Ionization

SELDI	Surface Enhanced Laser Desorption/Ionization
SIMS	Secondary Ion Mass Spectrometry
TOF	Time-Of-Flight
TOF-MS	Time-Of-Flight Mass Spectrometer

References

1 K. Deisewerd. The desorption process in MALDI. *Chem. Rev.* **2003**, *103*, 395–425.

2 M. Karas, R. Krüger. Ion formation in MALDI. *Chem. Rev.* **2003**, *103*, 427–439.

3 R. Knochenmuss, R. Zenobi. MALDI ionization: The role of in-plume processes. *Chem. Rev.* **2003**, *103*, 441–452.

4 H.D. Beckey. *Principles of Field Ionization and Field Desorption Mass Spectrometry, International Series in Analytical Chemistry*. Pergamon Press, 1977.

5 A. Benninghoven, W. Sichtermann. Detection, identification and structural investigation of biologically important compounds by secondary ion mass spectrometry. *Anal. Chem.* **1978**, *50*, 1180–1184.

6 D. Zakett, A.E. Schoen, R.G. Cooks, P.H. Hemberger. Laser-desorption mass spectrometry/mass spectrometry and the mechanism of desorption ionization. *J. Am. Chem. Soc.* **1981**, *103*, 1295–1297.

7 D.F. Torgerson, R.P. Skrowonski, R.D: Macfarlane. New approach to the mass spectroscopy of non volatile compounds. *Biochem. Biophys. Res. Commun.* **1974**, *60*, 616–619.

8 G.P. Jonsson, A.B. Hedin, P.L. Håkansson, B.U.R. Sundqvist, B.G. Save, P.F. Nielsen, P. Roepstorff, K.E. Johansson, I. Kamensky, M.S. Lindberg. Plasma desorption mass spectrometry of peptides and proteins adsorbed on nitrocellulose. *Anal. Chem.* **1986**, *58*, 1084–1087.

9 R.E. Honig, R.J. Woolston. Laser induced emission of electrons, ions, and neutral atoms from solid surfaces. *Appl. Phys. Lett.* **1963**, *2*, 138–141.

10 N.C. Fenner, N.R. Daly, Laser used for mass analysis. *Rev. Sci. Instrum.* **1966**, *37*, 1068–1072.

11 F.J. Vastola, R.O. Mumma, A.J. Pirone. Analysis of organic salts by laser ionization. *Org. Mass Spectrom.* **1970**, *3*, 101–104.

12 N.A. Posthumus, P.G. Kistemaker, H.L.C. Meuzelaar, M.C. Ten Noever de Brauw. Laser desorption-mass spectrometry of polar nonvolatile bio-organic molecules. *Anal. Chem.* **1978**, *50*, 985–991.

13 F. Hillenkamp, R. Kaufmann, R. Nitsche, E. Unsöld. Laser microprobe mass analysis of organic materials. *Nature* **1975**, *256*, 119–120.

14 M. Karas, D. Bachmann, F. Hillenkamp. Influence of the wavelength in high-irradiance ultraviolet laser desorption mass spectrometry of organic molecules. *Anal. Chem.* **1985**, *57*, 2935–2939.

15 F. Hillenkamp. Laser desorption mass spectrometry. A review. In: A. Benninghoven, R.J. Colton, D.S. Simons, H.W. Werner (Eds.), *Secondary Ion Mass Spectrometry SIMS V. Springer Series in Chemical Physics*, Vol. 44., Springer-Verlag, Berlin (1986), pp. 471–475.

16 M. Karas, F. Hillenkamp. Laser desorption ionization of proteins with molecular masses exceeding 10 000 daltons. *Anal. Chem.* **1988**, *60*, 2299–2301.

17 K. Tanaka, H. Waki, Y. Ido, S. Akita, Y. Yoshida, T. Yoshida. Protein and polymer analyses up to m/z 100 000 by laser ionization time-of-flight mass spectrometry. *Rapid Commun. Mass Spectrom.* **1988**, *2*, 151–153.

18 M. Schürenberg, K. Dreisewerd, F. Hillenkamp. Laser desorption/ionization mass spectrometry of peptides and proteins with particle suspension matrixes. *Anal. Chem.* **1999**, *71*, 221–229.

19 J. Sunner, E. Dratz, Y.-C. Chen. Graphite surface-assisted laser desorption/ionization time-of-flight mass spectrometry of peptides and proteins from liquid solutions. *Anal. Chem.* **1995**, *67*, 4335–4342.

20 J. Wei, J.M. Buriak, G. Siuzdak. Desorption–ionization mass

spectrometry on porous silicon. *Nature* **1999**, *399*, 243–246.
21 S.A. Trauger, E.P. Go, Z. Shen, J.V. Apon, B.J. Compton, E.S.P. Bouvier, M.G. Finn, G. Siuzdak. High sensitivity and analyte capture with desorption/ionization mass spectrometry on silylated porous silicon. *Anal. Chem.* **2004**, *76*, 4484–4489.
22 K. Strupat, M. Karas, F. Hillenkamp. 2,5-Dihydroxybenzoic acid: a new matrix for laser desorption-ionization mass spectrometry. *Int. J. Mass Spectrom. Ion Proc.* **1991**, *111*, 89–102.
23 R.C. Beavis, J.N. Bridson. Epitaxial protein inclusion in sinapic acid crystals. *Appl. Phys.* **1993**, *26*, 442–447.
24 V. Horneffer. *Matrix-Analyt-Wechelwirkungen bei der Matrix-Unterstützten Laserdesorptions/ionisations Massenspektrometrie (MALDI-MS)*. Dissertation, University of Münster, 2002.
25 J. Kampmeier, K. Dreisewerd, M. Schürenberg, F. Hillenkamp. Investigations of 2,5-DHB and succinic acid as matrices for IR and UV MALDI: Part 1: UV and IR laser ablation in the MALDI process. *Int. J. Mass Spectrom. Ion Proc.* **1997**, *169/170*, 31–41.
26 V. Horneffer, K. Dreisewerd, H.-C. Lüdememann, F. Hillenkamp, M. Lage, K. Strupat. Is the incorporation of analytes into matrix crystals a prerequisite for matrix-assisted laser desorption/ionization mass spectrometry? A study of five positional isomers of dihydroxybenzoic acid. *Int. J. Mass Spectrom.* **1999**, *185/186/187*, 859–870.
27 V. Horneffer, A. Forsmann, K. Strupat, F. Hillenkamp, U. Kubitschek. Localization of analyte molecules in MALDI preparations by confocal laser scanning microscopy. *Anal. Chem.* **2001**, *73*, 1016–1022.
28 R. Krueger, A. Pfenninger, I. Fournier, M. Glückmann, M. Karas. Analyte incorporation and ionization in matrix-assisted laser desorption/ionization visualized by pH indicator molecular probes. *Anal. Chem.* **2001**, *73*, 5812–5821.
29 V. Horneffer, R. Reichelt, K. Strupat. Protein incorporation into MALDI-matrix crystals investigated by high resolution field emission scanning electron microscopy. *Int. J. Mass Spectrom.* **2003**, *226*, 117–131.
30 R. Skelton, F. Dubois, R. Zenobi. A MALDI sample preparation method suitable for insoluble polymers. *Anal. Chem.* **2000**, *72*, 1707.
31 V. Horneffer, M. Glückmann, R. Krüger, M. Karas, K. Strupat, F. Hillenkamp. Matrix-analyte-interaction in MALDI-MS: Pellet and nano-electrospray preparations. *Int. J. Mass Spectrom.* **2006**, *249/250*, 426–432.
32 H.-C. Lüdemann. *Matrix-assisted laser desorption/ionization (MALDI): Optical spectroscopy of matrix molecules*. Dissertation, University of Münster, 2000, pp. 11–18.
33 H.-C. Lüdemann, R.W. Redmond, F. Hillenkamp. Singlet-singlet annihilation in UV-MALDI studied by fluorescence spectroscopy. *Rapid Commun. Mass Spectrom.* **2002**, *16*, 1287–1294.
34 R. Knochenmuss. Photoionization pathways and free electrons in UV-MALDI. *Anal. Chem.* **2004**, *76*, 3179–3184.
35 A. Rohlfing, Ch. Menzel, L.M. Kukreja, F. Hillenkamp, K. Dreisewerd. Photoacoustic analysis of matrix-assisted laser desorption/ionization processes with pulsed infrared lasers. *J. Phys. Chem. B* **2003**, *107*, 12275–12286.
36 A. Leisner, A. Rohlfing, U. Röhling, K. Dreisewerd, F. Hillenkamp. Time-resolved imaging of the plume dynamics in infrared matrix-assisted laser desorption/ionization with a glycerol matrix. *J. Phys. Chem. B* **2005**, *109*, 11661–11666.
37 Menzel, Ch., K. Dreisewerd, St. Berkenkamp, F. Hillenkamp. The role of the laser pulse duration in infrared matrix-assisted laser desorption/ionization mass spectrometry. *J. Am. Soc. Mass Spectrom.* **2002**, *13*, 975–984.
38 A. Rohlfing. *Untersuchungen zum Desorptionsprozess in der UV-Matrix-unterstützten Laserdesorptions/-ionisation mit einer Flüssigmatrix*. Dissertation, University of Münster, 2006.
39 A. Vogel, V. Venugopalan. Mechanisms of pulsed laser ablation of biological

tissues. *Chem. Rev.* **2003**, *103*, 577–644.

40 L.V. Zhigilei, B.J. Garrison. Mechanisms of laser ablation from molecular dynamics simulation: dependence on the initial temperature and pulse duration. *Appl. Phys. A* **1999**, *69*, 75–80.

41 L.V. Zhigilei, B. Garrison. Microscopic mechanisms of laser ablation of organic solids in the thermal and stress confinement irradiation regimes. *J. Appl. Phys.* **2000**, *88*, 1281–1298.

42 R. Knochenmuss, F. Dubois, M.J. Dale, R. Zenobi. The matrix suppression effect and ionization mechanisms in matrix-assisted laser desorption/ionization. *Rapid Commun. Mass Spectrom.* **1996**, *10*, 871–877.

43 M. Karas, D. Bachmann, U. Bahr, F. Hillenkamp. Matrix-assisted ultraviolet laser desorption of non-volatile compounds. *Int. J. Mass Spectrom. Ion Proc.* **1987**, *78*, 53–68.

44 H. Ehring, M. Karas, F. Hillenkamp. Role of photoionization and photochemistry in ionization processes of organic molecules and relevance for matrix-assisted laser desorption ionization mass spectrometry. *Org. Mass Spectrom.* **1992**, *27*, 472–480.

45 M. Karas, M. Glückmann, J. Schäfer. Ionization in matrix-assisted laser desorption/ionization: singly charged molecular ions are the lucky survivors. *J. Mass Spectrom.* **2000**, *35*, 1–12.

46 R.D. Burton, C.H. Watson, J.R. Eyler, G.L. Lang, D.H. Powell, M.Y. Avery. Proton affinities of eight matrices used for matrix-assisted laser desorption/ionization. *Rapid Commun. Mass Spectrom.* **1997**, *11*, 443–446.

47 A.G. Harrison. The gas-phase basicities and proton affinities of amino acids and peptides. *Mass Spectrom. Rev.* **1997**, *17*, 201–217.

48 R. Knochenmuss. A quantitative model of ultraviolet matrix-assisted laser desorption/ionization. *J. Mass Spectrom.* **2002**, *37*, 867–877.

49 R. Knochenmuss. A quantitative model of ultraviolet matrix-assisted laser desorption/ionization including analyte ion generation. *Anal. Chem.* **2003**, *75*, 2199–2207.

50 R. Krüger, M. Karas. Formation and fate of ion pairs during MALDI analysis: anion adduct generation as an indicative tool to determine ionization processes. *J. Am. Soc. Mass Spectrom.* **2002**, *13*, 1218–1226.

51 A. Pfenninger, M. Karas, B. Finke, B. Stahl, G. Sawatzki. Matrix optimization for matrix-assisted laser desorption/ionization mass spectrometry of oligosaccharides from human milk. *J. Mass Spectrom.* **1999**, *34*, 98–104.

52 M. Karas, U. Bahr, F. Hillenkamp, A. Tsarbopoulos, B.N. Pramanik. Matrix dependence of metastable fragmentation of glycoproteins in MALDI TOF mass spectrometry. *Anal. Chem.* **1995**, *67*, 675–679.

53 B. Spengler, D. Kirsch, R. Kaufmann. Fundamental aspects of post-source decay in MALDI mass spectrometry. *J. Phys. Chem.* **1992**, *96*, 9678–9684.

54 B. Spengler, D. Kirsch, R. Kaufmann. Metastable decay of peptides and proteins in matrix-assisted laser desorption mass spectrometry. *Rapid Commun. Mass Spectrom.* **1991**, *5*, 198.

55 B. Spengler. Post-source decay analysis in matrix-assisted laser desorption/ionization mass spectrometry of biomolecules. *J. Mass Spectrom.* **1997**, *32*, 1019–1036.

56 P. Chaurand, F. Luetzenkirchen, B. Spengler. Peptide and protein identification by matrix-assisted laser desorption ionization (MALDI) and MALDI-post-source decay time-of-flight mass spectrometry. *J. Am. Soc. Mass Spectrom.* **1999**, *10*, 91–103.

57 V. Gabelica, E. Schulz, M. Karas. Internal energy build-up in matrix-assisted laser desorption/ionization. *J. Mass Spectrom.* **2004**, *39*, 579–593.

58 E. Schulz, M. Karas, F. Rosu, V. Gabelica. Influence of the matrix on analyte fragmentation in atmospheric pressure MALDI. *J. Am. Soc. Mass Spectrom.* **2006**, *17*, 1005–1013.

59 U. Bahr, J. Stahl-Zeng, E. Gleitsmann, M. Karas. Delayed extraction time-of-flight MALDI mass spectrometry of proteins above 25 000 Da. *J. Mass Spectrom.* **1997**, *32*, 1111–1116.

60 M. Glückmann, M. Karas. The initial velocity and its dependence on matrix, analyte and preparation method in ultraviolet matrix-assisted laser desorption/ionization. *J. Mass Spectrom.* **1999**, *34*, 467–477.

61 R.S. Brown, J.L. Lennon. Sequence-specific fragmentation of matrix-assisted laser-desorbed protein/peptide ions. *Anal. Chem.* **1995**, *67*, 3990–3999.

62 R.S. Brown, B.L. Carr, J.L. Lennon. Factors that influence the observed fast fragmentation of peptides in matrix-assisted laser desorption. *J. Am. Soc. Mass Spectrom.* **1996**, *7*, 225–232.

63 M.N. Takayama. N-C bond cleavage of the peptide backbone via hydrogen abstraction. *J. Am. Soc. Mass Spectrom.* **2001**, *12*, 1044–1049.

64 M. Takayama. In-source decay characteristics of peptides in MALDI TOF mass spectrometry. *J. Am. Soc. Mass Spectrom.* **2001**, *12*, 420–427.

65 R.S. Brown, J. Feng, D.C. Reiber. Further studies of in-source fragmentation of peptides in MALDI. *Int. J. Mass Spectrom. Ion Proc.* **1997**, *169/170*, 1–18.

66 T. Köcher, A. Engström, R.A. Zubarev. Fragmentation of peptides in MALDI in-source decay mediated by hydrogen radicals. *Anal. Chem.* **2005**, *77*, 172–177.

67 D.C. Reiber, T.A. Grover, R.S. Brown. Identifying proteins using matrix-assisted laser desorption/ionization in-source fragmentation data combined with database searching. *Anal. Chem.* **1998**, *70*, 673–683.

68 M. Takayama, A. Tsugita. Sequence information of peptides and proteins with in-source decay in matrix assisted laser desorption/ionization-time of flight-mass spectrometry. *Electrophoresis* **2000**, *21*, 1670–1677.

69 B. Rosinke, K. Strupat, F. Hillenkamp, J. Rosenbusch, N. Dencher, U. Krüger, H.-J. Galla. Matrix-assisted laser desorption/ionization mass spectrometry (MALDI-MS) of membrane proteins and non-covalent complexes. *J. Mass Spectrom.* **1995**, *30*, 1462–14.

70 L.H.R. Cohen, K. Strupat, F. Hillenkamp. Analysis of quarternary protein ensembles by matrix-assisted laser desorption/ionization mass spectrometry. *J. Am. Soc. Mass Spectrom.* **1997**, *8*, 1046–1052.

71 Horneffer, K. Strupat, F. Hillenkamp. Localization of noncovalent complexes in MALDI-preparations by CLSM. *J. Am. Soc. Mass Spectrom.* (in press).

72 A. Wortmann, T. Pimenova, R. Zenobi. Investigation of the first shot phenomenon in MALDI mass spectrometry of protein complexes. 54th ASMS Conference on Mass Spectrometry and Allied Topics, Seattle, WA, May 28–June 1, 2006, Poster WP 256.

73 P. Juhasz, K. Biemann. Mass spectrometric molecular weight determination of highly acidic compounds of biological significance via their complexes with basic peptides. *Proc. Natl. Acad. Sci. USA* **1994**, *91*, 4333–4337.

74 M. Moniatte, F.G. van der Goot, J.T. Buckle, F. Pattus, A. van Dorsselaer. Characterisation of the heptameric pore-forming complex of the *Aeromonas* toxin aerolysin using MALDI-TOF mass spectrometry. *FEBS Lett.* **1996**, *384*, 269–272.

75 M.O. Glocker, S.H.J. Bauer, J. Kast, J. Volz, M. Przybylski. Characterization of specific noncovalent protein complexes by UV matrix-assisted laser desorption ionization mass spectrometry. *J. Mass Spectrom.* **1996**, *31*, 1221–1227.

76 I. Gruic-Sovulj, H.C. Lüdemann, F. Hillenkamp, I. Weygand-Duraseciv, Z. Kucan, J. Peter-Katalinic. Detection of noncovalent tRNA aminoacyl-tRNA synthetase complexes by matrix-assisted laser desorption/ionization mass spectrometry. *J. Biol. Chem.* **1997**, *272*, 32084–32091.

77 T. Vogl. J. Roth, F. Hillenkamp, K. Strupat. Calcium-induced non-covalently linked tetramers of MRP8 and MRP14 detected by ultraviolet matrix-assisted laser desorption/ionization mass spectrometry. *J. Am. Soc. Mass Spectrom.* **1999**, *10*, 1124–1130.

78 J.G. Kiselar, K.M. Downard. Preservation and detection of specific antibody-peptide complexes by matrix-assisted laser desorption ionization mass spectrometry. *J. Am. Soc. Mass Spectrom.* **2000**, *11*, 746–750.

79 A.S. Woods, M.A. Huestis. A study of peptide-peptide interaction by matrix-

assisted laser desorption/ionization. *J. Am. Soc. Mass Spectrom.* **2001**, *12*, 88–96.
80 A.S. Woods, J.M. Koomen, B.T. Ruotolo, K.J. Gillig, D.H. Russel, K. Fuhrer, M. Gonin, T.F. Egan, J.A. Schultz. A study of peptide-peptide interactions using MALDI ion mobility o-TOF and ESI mass spectrometry. *J. Am. Soc. Mass Spectrom.* **2002**, *13*, 166–169.
81 S.H. Luo, Y.M. Li, W. Qiang, Y.F. Zhao, H. Abe, T. Nemoto, X.R. Qin, H. Nakanishi. Detection of specific noncovalent interaction of peptide with DNA by MALDI-TOF. *J. Am. Soc. Mass Spectrom.* **2004**, *15*, 28–31.
82 M. Karas, U. Bahr, A. Ingendoh, F. Hillenkamp. Laser desorption/ionization mass spectrometry of proteins of mass 100 000 to 250 000 Dalton. *Angew. Chem. Int. Ed. Engl.* **1989**, *28*, 760–761.
83 F. Hillenkamp, M. Karas, R.C. Beavis, B.T. Chait. Matrix-assisted laser desorption ionization mass spectrometry of biopolymers. *Anal. Chem.* **1991**, *63*, 1193A–1203A.
84 F. Hillenkamp. *New methods for the study of biomolecular complexes; NATO ASI Series C: Mathematical and Physical Science 510.* Kluwer Academic Publishers: Dordrecht, The Netherlands, 1998; pp. 181–191.
85 T.B. Farmer, R.M. Caprioli. Determination of protein-protein interactions by matrix-assisted laser desorption/ionization mass spectrometry. *J. Mass Spectrom.* **1998**, *33*, 697–704.
86 M. Zehl, G. Allmaier. Instrumental parameters in MALDI-TOF mass spectrometric analysis of quaternary protein structures. *Anal. Chem.* **2005**, *77*, 103–110.
87 P. Lecchi, L.K. Pannelle. The detection of intact double-stranded DNA by MALDI. *J. Am. Soc. Mass Spectrom.* **1995**, *6*, 972–975.
88 F. Kirpekar, S. Berkenkamp, F. Hillenkamp. Detection of double-stranded DNA by IR- and UV-MALDI mass spectrometry. *Anal. Chem.* **1999**, *71*, 2334–2339.
89 J. Villanueva, O. Yanes, E. Querol, L. Serrano, F.X. Aviles. Identification of protein ligands in complex biological samples using intensity-fading MALDI-TOF mass spectrometry. *Anal. Chem.* **2003**, *75*, 3385–3395.
90 O. Yanes, J. Villanueva, E. Querol, F.X. Aviles. Functional screening of serine protease inhibitors in the medical leech *Hirudo medicinalis* monitored by intensity fading MALDI-TOF MS. *Mol. Cell. Proteomics* **2005**, *4*, 1602–1613.
91 O. Vorm, P. Roepstorff, M. Mann. Improved resolution and very high sensitivity in MALDI-TOF of matrix surfaces made by fast evaporation. *Anal. Chem.* **1994**, *66*, 3281–3287.
92 M. Schuerenberg, C. Luebbert, H. Eickhoff, M. Kalkum, H. Lehrach, E. Nordhoff. Prestructured MALDI-MS sample supports. *Anal. Chem.* **2000**, *72*, 3436–3442.
93 M. Karas, H. Ehring, E. Nordhoff, B. Stahl, K. Strupat, F. Hillenkamp, M. Grehl, B. Krebs. Matrix-assisted laser desorption/ionization mass spectrometry with additives to 2,5-dihydroxybenzoic acid, *Org. Mass Spectrom.* **1993**, *28*, 1476–1481.
94 Y.F. Zhu, C.N. Chung, N.I. Taranenko, S.L. Allman, S.A. Martin, L. Haff, C.H. Chen. The study of 2,3,4-trihydroxyacetophenone and 2,4,6-trihydroxyacetophenone as matrices for DNA detection in matrix-assisted laser desorption/ionization time-of-flight mass spectrometry. *Rapid Commun. Mass Spectrom.* **1996**, *10*, 383–388.
95 U. Pieles, W. Zürcher, M. Schär, H.E. Moser. Matrix-assisted laser desorption ionization time-of-flight mass spectrometry: a powerful tool for the mass and sequence analysis of natural and modified oligonucleotides. *Nucleic Acids Res.* **1993**, *21*, 3191–3196.
96 I. Smirnov, X. Zhu, T. Taylor, Y. Huang, P. Ross, I.A. Papayanopoulos, S.A. Martin, D.J. Pappin. Suppression of alpha-cyano-4-hydroxycinnamic acid matrix clusters and reduction of chemical noise in MALDI-TOF mass spectrometry. *Anal. Chem.* **2004**, *76*, 2958–2965.
97 S. Kjellström, O.N. Jensen. Phosphoric acid as a matrix additive for MALDI MS analysis of phosphopeptides and phosphoproteins. *Anal. Chem.* **2004**, *76*, 5109–5117.
98 A. Steensballe, O.N. Jensen. Phosphoric acid enhances the performance of

Fe(III) affinity chromatography and matrix-assisted laser desorption/ ionization tandem mass spectrometry for recovery, detection and sequencing of phosphopeptides. *Rapid Commun. Mass Spectrom.* **2004**, *18*, 1721–1730.

99 M.R. Larsen, T.E. Thingholm, O.N. Jensen, P. Roepstorff, J.D. Jorgensen. Highly selective enrichment of phosphorylated peptides from peptide mixtures using titanium dioxide microcolumns. *Molec. Cell Proteomics* **2005**, *4*, 873–886.

100 C.T. Chen, Y.-C. Chen. Fe_3O_4/TiO_2 core/shell nanoparticles as affinity probes for the analysis of phosphopeptides using TiO_2 surface-assisted laser desorption/ionization mass spectrometry. *Anal. Chem.* **2005**, *77*, 5912–5919.

101 D.W. Armstrong, L.K. Zhang, L. He, M.L. Gross. Ionic liquids as matrixes for matrix-assisted laser desorption/ionization mass spectrometry. *Anal. Chem.* **2001**, *73*, 3679–3686.

102 A. Tholey, E. Heinze. Ionic (liquid) matrices for matrix-assisted laser desorption/ionization mass spectrometry-applications and perspectives. *Anal. Bioanal. Chem.* **2006**, *386*, 24–37.

103 S. Trimpin, S. Keune, H.J. Rader, K. Mullen. Solvent-free MALDI-MS: developmental improvements in the reliability and the potential of MALDI in the analysis of synthetic polymers and giant organic molecules. *J. Am. Soc. Mass Spectrom.* **2006**, *17*, 661–671.